PERGAMON

Available online at www.sciencedirect.com

SCIENCE DIRECT®

Polyhedron 22 (2003) 1051–1057

POLYHEDRON

www.elsevier.com/locate/poly

The interaction of 2-methyllactic acid (H_2mL) with divalent metal cations. The structures of $[M(HmL)_2(H_2O)_2]$, M = Mn(II), Zn(II)

Rosa Carballo[a,*], Berta Covelo[a], Emilia García-Martínez[a], Ezequiel M. Vázquez-López[a], Alfonso Castiñeiras[b], Juan Niclós[c]

[a] Departamento de Química Inorgánica, Facultad de Ciencias, Universidad de Vigo, E-36200 Vigo, Galicia, Spain
[b] Departamento de Química Inorgánica, Facultad de Farmacia, Universidad de Santiago de Compostela, E-15706 Santiago de Compostela, Galicia, Spain
[c] Departamento de Química Inorgánica, Facultad de Farmacia, Universidad de Granada, E-18071 Granada, Spain

Received 4 October 2002; accepted 17 January 2003

Abstract

The mononuclear complexes $[M(HmL)_2(H_2O)_2]$, where M = Mn(II) (**1**), Ni(II) (**2**) or Zn(II) (**3**) and HmL = 2-methyllactato, were prepared and characterized by elemental analysis, FT-IR and UV/Vis spectroscopy and room temperature magnetic susceptibility measurements. Their thermal behaviour was also investigated, and compounds **1** and **3** were characterized by X-ray diffractometry. In both cases, the metal ion is hexacoordinated to two (O,O′)-bidentate monoanionic 2-methyllactato ligands and two aqua ligands in a distorted octahedral fashion. The $[M(HmL)_2(H_2O)_2]$ units are connected by hydrogen bonds, forming a two-dimensional network.

Keywords: Manganese(II); Nickel(II); Zinc(II); Crystal structures; 2-Methyllactato complexes; Thermal analysis

1. Introduction

Natural evolution has harnessed many metal ions for widely different essential biological functions. The interaction of these ions with biologically active ligands is a subject of considerable interest. Many such ligands are known to chelate metals [1], but often little is known about exactly how metal binding influences their biological activity. α-Hydroxycarboxylic acids are involved in several biochemical processes and are also frequently used in pharmaceutical formulations. Coordination to these redox-inert ligands seems to be essential for both the mobilization and the reduction of certain metal ions in vivo; for example, they are thought to play important roles in iron metabolism and in the incorporation of vanadium and molybdenum in the active site of nitrogenases [2]. Certain metal complexes of these ligands also have medicinal properties [3–5].

As a contribution to understanding the chemistry of divalent metal ions in the presence of α-hydroxyacids, in this work we studied the interaction of three essential metal ions (manganese(II), nickel(II) and zinc(II)) with 2-methyllactic acid (H_2mL) (see Scheme 1).

Previous work in this area has mostly concerned the solid state coordination behaviour of manganese and zinc with glycolic and lactic acids (H_2Gly and H_2Lac, respectively); this work has led to the isolation of the complexes $[Mn(HGly)_2(H_2O)_2]$ [6,7], $[Mn(HLac)_2(H_2O)_2]$ [8], $[Mn(HLac)_2(H_2O)_2]\cdot H_2O$ [9,10] and $(TMA)_3[Mn_2(Lac)_4(HLac)]\cdot H_2O$ (TMA = tetramethylammonium) [11] and of $[Zn(HGly)_2(H_2O)_2]$ [12], $[Zn(HLac)_2(H_2O)_2]\cdot H_2O$ [13] and $[Zn(HLac)_2]_\infty$ [14] (this last obtained by a hydrothermal method). However, to the best of our knowledge the only previously reported Mn, Ni or Zn complex of 2-methyllactic acid (H_2mL) is the Mn(IV) compound $Na_3[NaMn_2(mL)_6]\cdot 4MeOH$ [11].

---

* Corresponding author. Tel.: +34-986-812-273; fax: +34-986-813-798.

E-mail address: rcrial@uvigo.es (R. Carballo).

0277-5387/03/$ - see front matter © 2003 Elsevier Science Ltd. All rights reserved.
doi:10.1016/S0277-5387(03)00090-1

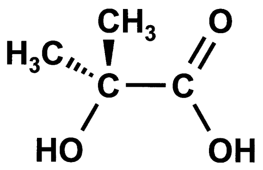

Scheme 1.

2. Experimental

2.1. Physical measurements

Microanalyses (C, H) were carried out with a FISONS EA-1108 elemental analyser. Melting points (m.p.) were measured with a Gallenkamp MBF-595 apparatus. FT-IR spectra in the 4000–400 cm^{-1} region were recorded from KBr pellets on a Bruker VECTOR 22 spectrometer. A Shimadzu UV-3101PC spectrophotometer was used to obtain the electronic spectra of **1** and **2** in the region 250–900 nm. Magnetic susceptibility measurements on **1** and **2** were performed at 25 °C using a Johnson Matthey Alfa MSB-MKI Gouy balance. TG/DTG analysis profiles (pyrolysis, 300–1000 K, with IR and MS investigation of evolved gases) were recorded under a 100 ml min^{-1} air flow using a Shimadzu TGA-DTG-50H Thermobalance coupled to a Nicolet Magma 550 FT-IR apparatus and a Fisons Thermolab mass spectrometer. Powder X-ray diffraction data obtained using Cu Kα radiation were collected on a Siemens D-5000 diffractometer over the range 5.0°–45.0° in steps of 0.20° (2θ) with a count time per step of 5.0 s.

2.2. Materials

All reagents and solvents were obtained commercially, 2-methyllactic acid (H_2mL) from Fluka, $Mn(AcO)_2$ from Panreac and $Ni(AcO)_2 \cdot 4H_2O$ and $ZnCO_3$ from Probus. All were used as supplied.

2.2.1. Synthesis of the complexes

*2.2.1.1. $[Mn(HmL)_2(H_2O)_2]$ (**1**).* A solution of 2-methyllactic acid (2.23 mmol) in 10 ml of ethanol was slowly added to a solution of $Mn(AcO)_2$ (1.11 mmol) in 10 ml of the same solvent. The white suspension so obtained was stirred at room temperature for 3 days and the resulting white solid was filtered off, washed with ethanol and dried in vacuo. Recrystallisation in water allowed the isolation of single crystals of **1**.

Yield 60%. M.p. > 250 °C. *Anal.* Found: C, 32.0; H, 6.1. Calc. for $C_8H_{18}O_8Mn$ (297.16): C, 32.4; H 6.1%. IR (KBr, ν/cm^{-1}): ν(OH) 3404s, 3168s; ν_{as}(OCO) 1632s; ν_s(OCO) 1487m; ν(C–OH) 1165s. UV–Vis (ν/cm^{-1}): 29 400, 23 250. μ_{eff} (298 K, M.B.): 5.71.

*2.2.1.2. $[Ni(HmL)_2(H_2O)_2]$ (**2**).* A solution of 2-methyllactic acid (2.01 mmol) in 10 ml of ethanol was slowly added to a solution of $Ni(AcO)_2 \cdot 4H_2O$ (1.00 mmol) in 10 ml of water. The green suspension so obtained was heated for 10 min, after which magnetic stirring at room temperature was maintained for several days. The green crystalline powder formed was filtered off, washed with ethanol and dried in vacuo.

Yield 43%. M. p. > 250 °C. *Anal.* Found: C, 32.0; H, 6.2. Calc. for $C_8H_{18}O_8Ni$ (300.92): C, 31.9; H, 6.5%. IR (KBr, ν/cm^{-1}): ν(OH) 3448s, 3193s; ν_{as}(OCO) 1624s, ν_s(OCO) 1487m; ν(C–OH) 1174s. UV–Vis (ν/cm^{-1}): 25 252, 15 015(13 624), 8695(7547). μ_{eff} (298 K, M.B.): 3.37.

*2.2.1.3. $[Zn(HmL)_2(H_2O)_2]$ (**3**).* A solution of 2-methyllactic acid (2.05 mmol) in 10 ml of ethanol was slowly added to a suspension of $ZnCO_3$ (1.02 mmol) in 10 ml of water. Magnetic stirring was maintained at room temperature for a week. The white solid formed was filtered off, washed with ethanol and water and dried in vacuo. Colourless single crystals of **3** suitable for X-ray diffraction studies were obtained by slow concentration of the filtrate.

Yield 76%. M.p. > 250 °C. *Anal.* Found: C, 31.0; H, 5.7. Calc. for $C_8H_{18}O_8Zn$ (307.61): C, 31.2; H, 5.9%. IR (KBr, ν/cm^{-1}): ν(OH) 3433s, 3178s; ν_{as}(OCO) 1631s; ν_s(OCO) 1491m; ν(C–OH) 1171s.

2.3. X-ray data collection and reduction

Crystallographic data for **1** and **3** were collected on a Bruker Smart CCD diffractometer at 293 K using graphite-monochromated Mo Kα radiation ($\lambda = 0.71073$ Å). The data were corrected for Lorentz and polarization effects, and also, using the program SADABS [15], for absorption. The structures were solved by direct methods using the program SHELXS-97 [16]. All non-hydrogen atoms were refined with anisotropic thermal parameters by full-matrix least-squares calculations on F^2 using the program SHELXL-97 [17]. Hydrogen atoms were inserted at calculated positions and constrained with isotropic thermal parameters, except for those of the hydroxyl groups and water molecules, which were located using a Fourier difference map and refined isotropically. For **3**, which crystallized in the chiral space group $P3_221$, the analysis established unambiguously the absolute stereochemistry of the complex [Flack parameter 0.00(5)]. Drawings were produced with ZORTEP [18] and SCHAKAL [19]. Crystal data and structure refinement parameters are listed in Table 1.

Table 1
Crystal data and structure refinement for $[Mn(HmL)_2(H_2O)_2]$ (**1**) and $[Zn(HmL)_2(H_2O)_2]$ (**3**)

Compound	**1**	**3**
Empirical formula	$C_8H_{18}O_8Mn$	$C_8H_{18}O_8Zn$
Formula weight	297.16	307.61
Crystal size (mm)	0.36 × 0.36 × 0.20	0.15 × 0.12 × 0.06
Crystal system	monoclinic	trigonal
Space group	*C*2/*c* (no. 15)	*P*3$_2$21 (no. 154)
a (Å)	10.2316(10)	5.8402(15)
b (Å)	5.7454(5)	5.8402(15)
c (Å)	21.884(2)	31.816(11)
β (°)	101.464(2)	–
V (Å^3)	1260.8(2)	939.8(5)
Z	4	3
D_{calc} (Mg m^{-3})	1.566	1.631
F(000)	620	480
Range θ (°)	1.90–28.03	1.92–28.08
h_{min}/h_{max}	−9/13	−7/7
k_{min}/k_{max}	−7/7	−7/6
l_{min}/l_{max}	−28/28	−41/37
μ (mm^{-1})	1.073	1.987
Max/min transmissions	1.000/0.720	1.000/0.372
Reflections collected/unique	3898/1493	5980/1515
Data/parameters	1493/90	1515/91
Final R [$I > 2\sigma(I)$]	0.0350	0.0671
Final wR_2 [$I > 2\sigma(I)$]	0.0914	0.1402
GOF	1.226	1.000

3. Results and discussion

The complexes **1**, **2** and **3** were synthesized using 2-methyllactic acid and the metallic salts [$Mn(AcO)_2$, $Ni(AcO)_2 \cdot 4H_2O$ or $ZnCO_3$] in 2:1 mole ratio. Elemental analyses of the compounds led to their formulation as $[M(HmL)_2(H_2O)_2]$. The crystalline solids have proved to be stable in air for long periods of time without any visible decomposition, and are soluble in water but insoluble in common organic solvents. Single crystals suitable for X-ray diffractometry were obtained for **1** and **3**. Comparison of the observed XRD patterns of **1**, **2** and **3** showed that the nickel(II) and zinc(II) complexes are isomorphous (Fig. 1).

3.1. Thermal analysis

The TGA profiles (Fig. 2) show two distinct mass loss regions for **1** and **2**, and three for **3**. To investigate the species, we monitored the evolved gases by means of IR spectroscopy. The first mass loss region, (85–135 °C for **1**, 120–270 °C for **2** and 75–130 °C for **3**) is due to removal of coordinated H_2O; the observed mass losses, 12.02% (**1**), 12.17% (**2**) and 10.44% (**3**) correspond to respectively 1.8, 2 and 1.78 equiv. of H_2O per formula unit. The next mass loss (over the range 200–230 °C in **1**, 300–350 °C in **2** and at 250–370 °C in **3**) reflects the loss of one 2-methyllactato ligand from **3** or of both from **1** and **2**; the second 2-methyllactato ligand of **3** is lost between 370 and 400 °C. The observed residual weights, 28.7% (**1**), 26.8% (**2**) and 31.3% (**3**), are close to those expected for MnO_2 (29.3%), NiO (24.8%) and $Zn(OH)_2$ (32.3%), respectively.

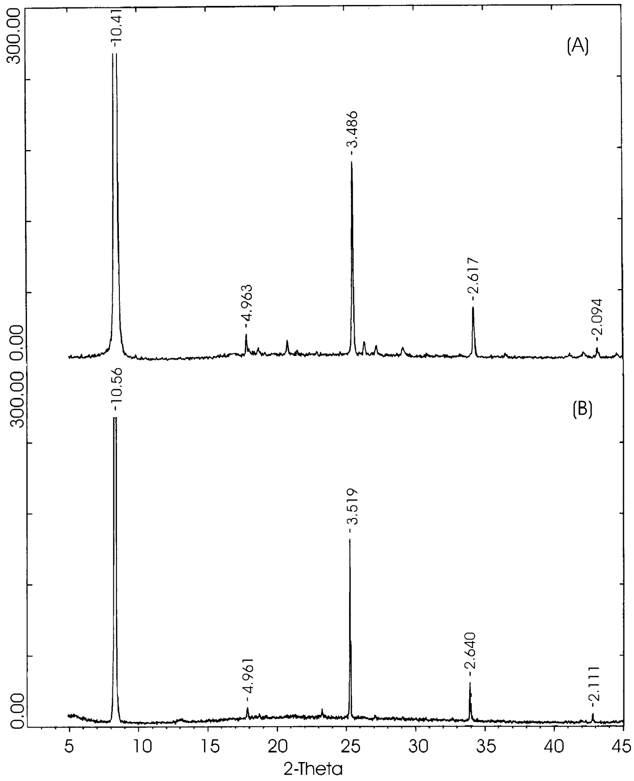

Fig. 1. Powder X-ray diffraction pattern of **2** (A) and **3** (B).

3.2. Crystal structures

Selected interatomic distances and angles in **1** and **3**, and the geometric parameters of their main hydrogen bonds, are listed in Tables 2 and 3, respectively. Figs. 3 and 4 show drawings of their molecular structures together with the atom-numbering schemes used. Compound **1**, which is isotypic with $[Co(HmL)_2(H_2O)_2]$ [20], crystallises in the space group *C*2/*c*, with the manganese atom located on the twofold axis. Compound **3** crystallizes in the trigonal space group *P*3$_2$21 with the zinc atom located on a twofold axis (Wyckoff position a). The structures of both compounds are based on neutral $[M(HmL)_2(H_2O)_2]$ units, where HmL a monoanionic (O,O′)-bidentate 2-methyllactato ligand that chelates the divalent metallic cation through the carboxyl and hydroxyl oxygen atoms to form a five-membered chelate ring. In both, the two aqua ligands are *cis* to each other, and the coordination polyhedron is a distorted octahedron in which the main deviations from regularity affect the chelating angles $O_{hydroxyl}–M–O_{carboxy}$, 72.32(5)° in **1** and 75.98(18)° in **3**, (in **1** this angle is smaller than in the isotypic Co(II) complex, but similar to those observed in other aqua complexes of Mn(II) with α-hydroxycarbox-

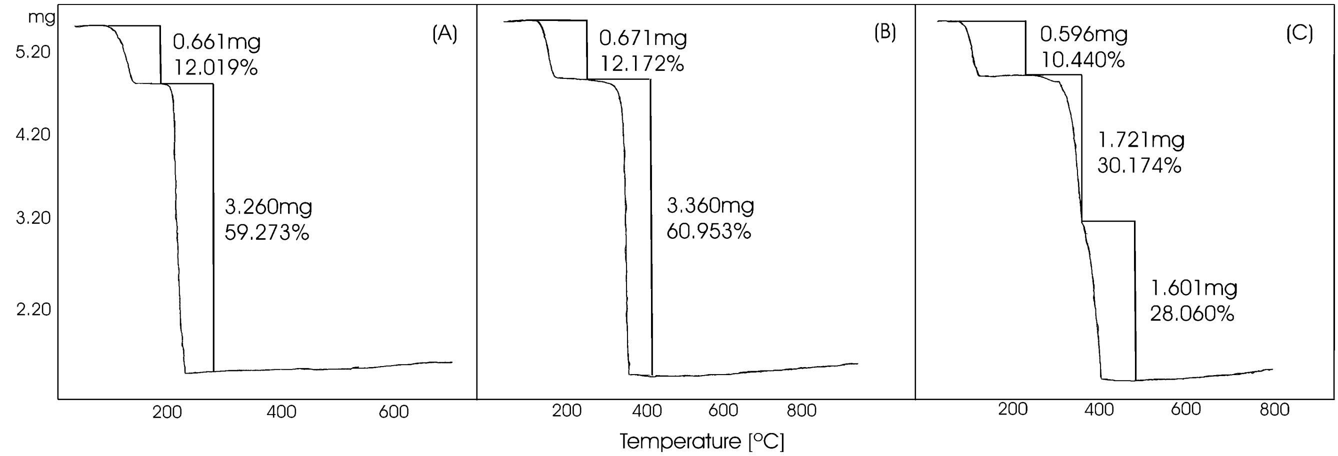

Fig. 2. Thermogravimetric analysis results for **1** (A), **2** (B) and **3** (C).

Table 2
Selected bond lengths (Å) and angles (°) for $[Mn(HmL)_2(H_2O)_2]$ (**1**) and $[Zn(HmL)_2(H_2O)_2]$ (**3**)

Compound	**1**	**3**
Bond lengths		
M–O(1)	2.1443(15)	2.064(6)
M–O(11)	2.1608(13)	2.076(5)
M–O(13)	2.1725(13)	2.087(4)
Bond angles		
O(1)–M–O(1)^{i}	86.76(10)	88.6(4)
O(1)–M–O(11)^{i}	92.92(7)	90.3(3)
O(1)–M–O(11)	155.82(6)	162.5(2)
O(11)^{i}–M–O(11)	97.00(8)	95.8(3)
O(1)–M–O(13)^{i}	106.97(7)	101.3(2)
O(11)–M–O(13)^{i}	97.06(6)	96.1(2)
O(1)–M–O(13)	84.64(6)	87.1(2)
O(11)–M–O(13)	72.32(5)	76.0(2)
O(13)^{i}–M–O(13)	164.32(9)	168.3(3)

Symmetry transformation used for generate equivalent atoms: $^{i}1-x, y, 3/2-z$ (**1**); $y, x, 2-z$ (**3**).

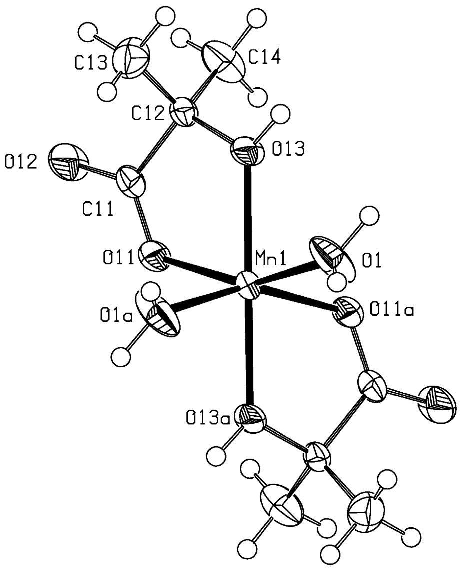

Fig. 3. Molecular structure of $[Mn(HmL)_2(H_2O)_2]$ (**1**), showing 50% probability displacement ellipsoids.

ylato ligands [7,8]). In both compounds the configuration around the metal atom is describable in the CPI system as OC-6-33 [21], with the priority order $O_{carboxy}$ (**1**) > $O_{hydroxyl}$ (**2**) > O_{water} (**3**); as in the Co(II) compound [20], the hydroxyl oxygen atoms are mutually *trans*.

All the coordinating bonds are shorter in the Zn(II) complex (**3**) than in the Mn(II) complex (**1**). The M–$O_{hydroxyl}$ bonds are just slightly longer than the M–$O_{carboxy}$ bonds. Although this difference is generally much larger [7,22], similar behaviour has been observed in other Mn(II) and Zn(II) α-hydroxycarboxylato complexes [8,13], and in $[Co(HmL)_2(H_2O)_2]$ Co–$O_{hydroxyl}$ is shorter than the Co–$O_{carboxy}$ [20]. The Mn–O_w, Mn–$O_{carboxy}$ and Mn–$O_{hydroxyl}$ bonds have lengths similar to those found in aqua complexes of Mn(II) with other α-hydroxycarboxylato ligands [6–8,10]. The Zn–$O_{carboxy}$ and Zn–$O_{hydroxyl}$ bonds are slightly shorter than in the similar compound $[Zn(HLac)_2(H_2O)_2]$ [12], and Zn–O_w

Table 3
Hydrogen bond distances (Å) and angles (°) for $[Mn(HmL)_2(H_2O)_2]$ (**1**) and $[Zn(HmL)_2(H_2O)_2]$ (**3**)

D–H···A	d(D–H)	d(H···A)	d(D···A)	∠(DHA)
$[Mn(HmL)_2(H_2O)_2]$ (**1**)				
O(13)–H(13)···O(12)^{i}	0.86(4)	1.85(4)	2.709(2)	178(3)
O(1)–H(1)···O(11)^{i}	0.92(3)	1.77(4)	2.696(2)	177(3)
O(1)–H(2)···O(11)^{ii}	0.73(3)	2.19(3)	2.896(2)	164(4)
$[Zn(HmL)_2(H_2O)_2]$ (**3**)				
O(13)–H(13)···O(12)^{i}	0.89(6)	1.80(6)	2.664(7)	164(6)
O(1)–H(1)···O(11)^{i}	0.80(8)	2.04(8)	2.722(7)	142(8)
O(1)–H(2)···O(11)^{ii}	0.87(10)	2.36(10)	3.036(9)	135(8)

Symmetry transformation used for generate equivalent atoms: $^{i}x+1/2, y+1/2, z$; $^{ii}-x+1, y+1, -z+3/2$ (**1**); $^{i}x-1, y, z$; $^{ii}y-1, x-1, 2-z$ (**3**).

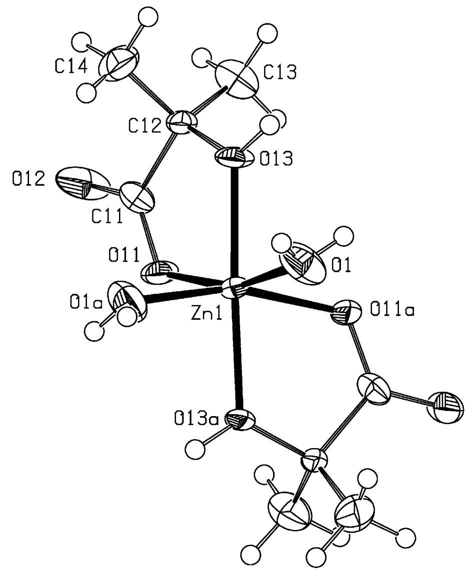

Fig. 4. Molecular structure of $[Zn(HmL)_2(H_2O)_2]$ (**3**), showing 50% probability displacement ellipsoids.

is intermediate in length between the two Zn–O_w bonds of this lactato complex, which likewise has two *cis* aqua ligands [12]. The carboxylate groups have clearly different C–O lengths [1.275(2) and 1.232(2) Å in **1**, 1.288(8) and 1.233(8) Å in **3**], suggesting that the bond between the carboxy carbon and the non-coordinating oxygen has significant double bond character.

In both compounds the nature of the ligand and the presence of two coordinated water molecules gives rise to the formation of a supramolecular architecture based on hydrogen bonding, specifically an infinite two-dimensional network similar to that observed in $[Co(HmL)_2(H_2O)_2]$ [20] (Fig. 5). There are three types of intermolecular hydrogen bonds (Table 3): one between $O_{hydroxyl}$ and the uncoordinated $O_{carboxy}$ atom (O···O range 2.66–2.71 Å), and two between the coordinated $O_{carboxy}$ and the aquo ligands (O···O range 2.69–3.04 Å); in all three cases the O···O distances are in the usual range for complexes with α-hydroxycarboxylato ligands [20,23]. Each molecule of the complex is thus involved in a total of twelve hydrogen bonds with six different adjacent molecules (Fig. 6).

However, the differences in the orientation and length of the interactions $O_{carboxy}\cdots O_w$ are responsible for the spontaneous resolution of the enantiomers in the Zn(II) complex in clear contrast with the Co(II) [20] and Mn(II) complexes which crystallize as racemates.

3.3. Infrared spectroscopy

The IR spectra of the complexes show two broad bands in the 3500–3100 cm^{-1} region corresponding to $\nu(OH)$. A strong band near 1630 cm^{-1} is attributable to the asymmetric COO^- stretching vibrations, and the band at 1487 cm^{-1} (**1** and **2**) or 1491 cm^{-1} (**3**) to $\nu_s(COO^-)$. The values of $[\nu_{as}(COO^-)-\nu_s(COO^-)]$ [24], 145 cm^{-1} for **1**, 137 cm^{-1} for **2** and 140 cm^{-1} for **3**, are smaller than expected for a monodentate carboxylato group. This is attributable to the 'pseudo-bridge'

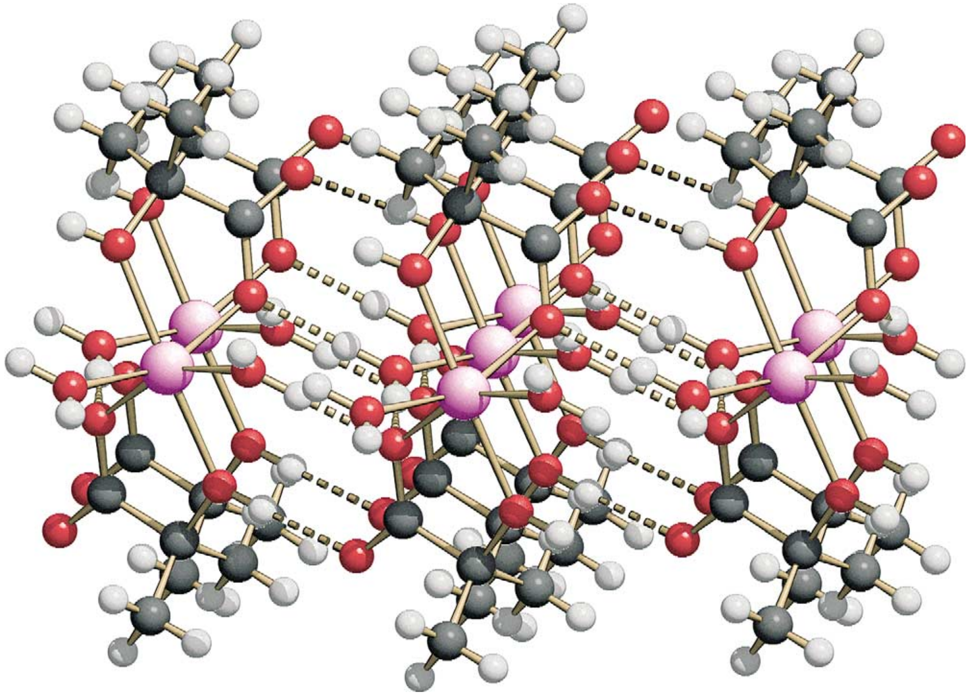

Fig. 5. Crystal packing diagram showing the molecules and hydrogen-bonded layers of $[Mn(HmL)_2(H_2O)_2]$ (**1**) running along the crystallographic *b*-axis.

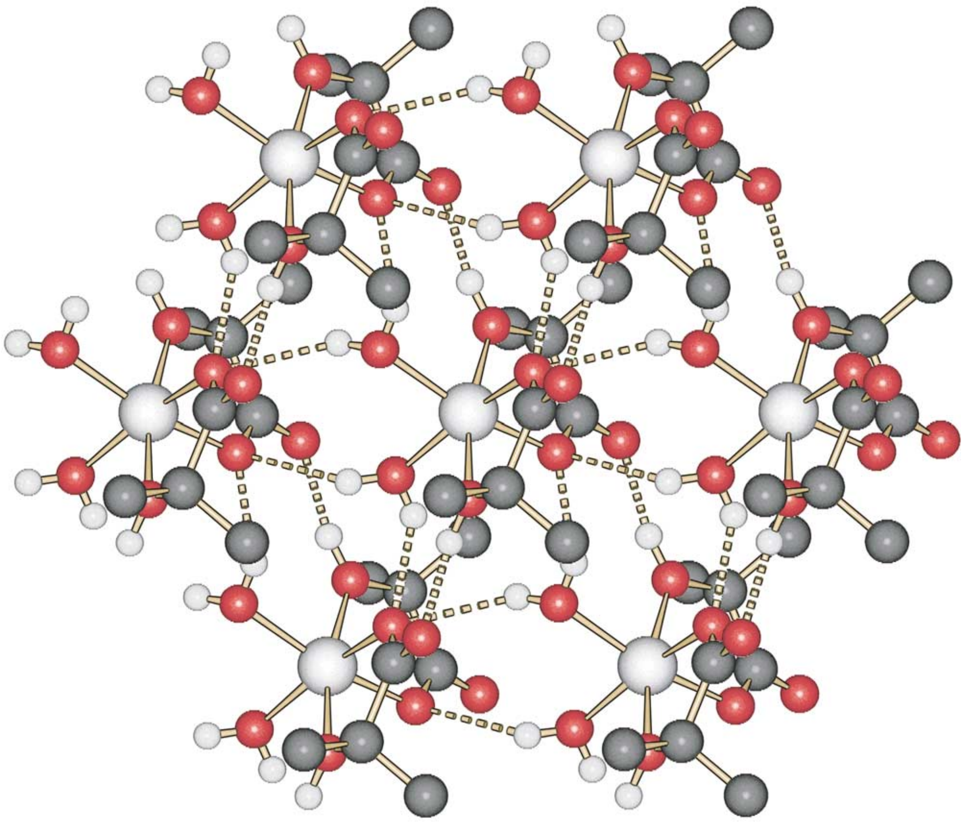

Fig. 6. A fragment of infinite 2D network through hydrogen bonds of [$Zn(HmL)_2(H_2O)_2$] (**3**) showing the close-packing of molecules in the plane *ac*.

behaviour [24] of a carboxylato group involved in a strong hydrogen bond through its uncoordinated oxygen (see X-ray results in Table 3). The above assignments are in agreement with results for the 2-methyllactato cobalt(II) aqua complex [20].

3.4. Electronic and magnetic properties

The room-temperature effective magnetic moment (μ_{eff}) of the Mn(II) and Ni(II) complexes (5.71 and 3.37 M.B. for **1** and **2**, respectively) agree rather well with the values predicted for the spin-free complexes [25]. The electronic spectrum of **1**, recorded in the solid state by diffuse reflectance is dominated by a band at 29 400 cm^{-1} probably associated with intraligand electronic transitions. The visible region of the spectrum displays a weak shoulder at 23 250 cm^{-1} ascribed to a ligand-to-metal charge-transfer transition from the 2-methyllactato oxygen atoms to an half-filled 3d orbital on the manganese(II). The diffuse-reflectance spectrum of the nickel(II) compound, with bands at 8690, 15 015 and 25 252 cm^{-1}, is typical of octahedral symmetry. Therefore, assignments of the observed absorption bands at $^3A_{2g} \rightarrow {}^3T_{2g}$ (ν_1), $^3A_{2g} \rightarrow {}^3T_{2g}(F)$ (ν_2), and $^3A_{2g} \rightarrow {}^3T_{2g}(P)$ (ν_3) transitions, respectively [26,27]. Using the appropriate equation [28] and the energy of the $^3A_{2g} \rightarrow {}^3T_{2g}(P)$ transition, a value of 14 812 cm^{-1} was calculated for the $^3A_{2g} \rightarrow {}^3T_{2g}(F)$ transition. This value compares favorably with the experimental value of 15 015 cm^{-1}.

4. Supplementary material

Supplementary crystallographic data are available from the Cambridge Crystallographic Data Centre, citing deposition numbers CCDC 189 255 and 189 256. Copies of this information may be obtained free of charge from The Director, CCDC, 12 Union Road, Cambridge, CB2 1EZ (fax: +44-1223-336033; e-mail: deposit@ccdc.cam.ac.uk or www: http://ccdc.cam.ac.uk).

Acknowledgements

Financial support with ERDF (EU) and DGI-MCYT (Spain) funds (research projects BQU2002-03543 and BQU2002-04523-C02) are gratefully acknowledged.

References

[1] A. Albert, Selective Toxicity. The Physico-Chemical Basis of Therapy, sixth ed., Chapman and Hall, London, 1979.

[2] M. Biagioli, L. Strinna-Erre, G. Micera, A. Panzanelli, M. Zema, Inorg. Chim. Acta 310 (2000) 1.

[3] P. Kiprof, W. Scherer, L. Pajdla, E. Herdtweck, W.A. Herrmann, Chem. Ber. 125 (1992) 43.

[4] G.G. Bombi, B. Corain, A.A. Sheikh-Osman, G.C. Valle, Inorg. Chim. Acta 171 (1990) 79.

[5] Z. Guo, P.J. Sadler, Angew. Chem., Int. Ed. Engl. 38 (1999) 1512.

[6] T. Lis, Acta Crystallogr., Sect. B 36 (1980) 701.

[7] G.G. Melikyan, F. Amiryan, M. Visi, K.I. Hardcastle, B.L. Bales, G. Aslanyan, S.H. Badanyan, Inorg. Chim. Acta 308 (2000) 45.

[8] T. Lis, Acta Crystallogr., Sect. B 38 (1982) 937.

[9] K.D. Singh, S.C. Jain, T.D. Sakore, A.B. Biswas, Z. Kristallogr. 141 (1975) 473.

[10] T. Kemmitt, A.M. Mills, G.J. Gainsford, Aust. J. Chem. 54 (2001) 37.

[11] S.M. Saadeh, M.S. Lah, V.L. Pecoraro, Inorg. Chem. 30 (1991) 8.

[12] A.J. Fischinger, L.E. Webb, J. Chem. Soc. D (1969) 407.

[13] K.D. Singh, S.C. Jain, T.D. Sakore, A.B. Biswas, Acta Crystallogr., Sect. B 31 (1975) 990.

[14] Z.-F. Chen, J. Zhang, R.-G. Xiong, X.-Z. You, Inorg. Chem. Comm. 3 (2000) 493.

[15] G.M. Sheldrick, SADABS, a Program for Absorption Correction, University of Göttingen, Göttingen, Germany, 1996.

[16] G.M. Sheldrick, SHELXS-97, a Program for the Solution of Crystal Structures from X-ray Data, University of Göttingen, Göttingen, Germany, 1997.

[17] G.M. Sheldrick, SHELXL-97, a Program for the Refinement of Crystal Structures from X-ray Data, University of Göttingen, Göttingen, Germany, 1997.

[18] L. Zsolnai, G. Huttner, ZORTEP, a Program for the Presentation of Thermal Ellipsoids, University of Freiburg, Freiburg, Germany, 1988.

[19] E. Keller, SCHAKAL-97, a Computer Program for the Graphic Representation of Molecular and Crystallographic Models, University of Freiburg, Freiburg, Germany, 1997.

[20] R. Carballo, A. Castiñeiras, B. Covelo, J. Niclós, E.M. Vázquez-López, Z. Anorg. Allg. Chem. 628 (2002) 468.

[21] A. Von Zelewsky, Stereochemistry of Coordination Compounds, Wiley, Chichester, 1996.

[22] M. Matzapetakis, N. Karligiano, A. Bino, M. Dakanali, C.P. Raptopoulou, V. Tangoulis, A. Terzis, J. Giapintzakis, A. Salifoglou, Inorg. Chem. 39 (2000) 4044.

[23] R. Carballo, A. Castiñeiras, B. Covelo, E.M. Vázquez-López, Polyhedron 20 (2001) 899.

[24] G.B. Deacon, R. Phillips, Coord. Chem. Rev. 33 (1980) 227.

[25] R.L. Carlin, Magnetochemistry, Springer, Berlin, 1986.

[26] A.B.P. Lever, Inorganic Electronic Spectroscopy, second ed., Elsevier, Amsterdam, 1984.

[27] L.J. Bostelaar, R.A.G. de Graaff, F.B. Hulsbergen, J. Reedijk, W.M.H. Sachtler, Inorg. Chem. 23 (1984) 2294.

[28] R.S. Drago, Physical Methods for Chemists, second ed., Saunders College Publishing, Orlando, FL,, 1992.